Sabolić I., Škarica M., Ljubojević M., Breljak D., Herak-Kramberger C.M., Crljen V., Ljubešić N. (2018) ***Expression and immunolocalization of metallothioneins MT1, MT2 and MT3 in rat nephron.*** **Journal of trace elements in medicine and biology, 46. pp. 62-75. ISSN 0946-672X**

http://www.elsevier.com/locate/issn/0946672X

http://www.sciencedirect.com/science/journal/0946672X

https://doi.org/10.1016/j.jtemb.2017.11.011

http://medlib.mef.hr/3392

Expression and immunolocalization of metallothioneins MT1, MT2 and MT3 in rat nephron[†]

Ivan Sabolić[a]* Mario Škarica[a§], Marija Ljubojević[a], Davorka Breljak[a], Carol M. Herak-Kramberger[a], Vladiana Crljen[b], Nikola Ljubešić[c]

[a]Molecular Toxicology Unit, Institute for Medical Research and Occupational Health; [b]Croatian Institute for Brain Research & Department of Physiology, School of Medicine, University of Zagreb; [c]Croatian Academy of Sciences and Arts (HAZU); Zagreb, Croatia

[§]Present address: Department of Neuroscience, Yale University School of Medicine, New Haven, CT, USA

***Corresponding author:**

Ivan Sabolić, MD, PhD

Molecular Toxicology Unit, Institute for Medical Research and Occupational Health

Ksaverska cesta 2, 10000 Zagreb, Croatia

Tel. +385-91-591-6746; Fax. +385-1-4673-303; E-mail: sabolic@imi.hr

Short Title: Metallothioneins in rat nephron

[†]The results of this paper were partially presented at XI. ISTERH Conference, Srebreno, Croatia 18–22 October 2015.

Abstract

Rodent kidneys exhibit three isoforms of metallothioneins (MTs), MT1, MT2 and MT3, with poorly characterized localization along the nephron. Here we studied in adult male Wistar rats the renal expression of *MTs* mRNA by end-point RT-PCR and MT proteins by immunochemical methods. The expression pattern of *MT1* mRNA was cortex (CO)>outer stripe (OS)=inner stripe (IS)=inner medulla (IM), of *MT2* mRNA was IM>CO>IS=OS, and of *MT3* mRNA was IM>CO=OS=IM. MT1/2-antibody stained with heterogeneous intensity the cell cytoplasm and nuclei in proximal tubule (PT) and thin ascending limb, whereas MT3-antibody stained weakly the cell cytoplasm in various cortical tubules and strongly the nuclei in all nephron segments. However, the isolated nuclei exhibited an absence of MT1/2 and presence of MT3 protein. In MT1/2-positive PT cells, the intracellular staining appeared diffuse or bipolar, but the isolated brush-border, basolateral and endosomal membranes were devoid of MT1/2 proteins. In the lumen of some PT profiles, the heterogeneously sized MT1/2-rich vesicles were observed, with the limiting membrane positive for NHE3, but negative for V-ATPase, CAIV, and megalin, whereas their interior was positive for CAII and negative for cytoskeleton. They seem to be pinched off from the luminal membrane of MT1/2-rich cells, as also indicated by transmission electron microscopy. We conclude that in male rats, MTs are heterogeneously abundant in the cell cytoplasm and/or nuclei along the nephron. The MT1/2-rich vesicles in the tubule lumen may represent a source of urine MT and membranous material, whereas MT3 in nuclei may handle zink and locally-produced reactive oxygen species.

Key words: immunocytochemistry, rat kidney, mRNA expression, proximal tubule, transmission electron microscopy, Western blotting

1. Introduction

Metallothioneins (MTs) are small (Mr = 6-8 kDa) cysteine rich proteins which bind Zn, Cd, and a few other toxic metals with variable affinity. In adult mammals, functional MTs exist in four isoforms. MT1 and MT2 (MT1/2) are widely expressed in different organs and in heterogeneous abundance [1], MT3 is found largely in brain, but also in a few other organs [2-6], whereas MT4 is found in some stratified squamous epithelia [7].

The exact functions of individual MTs have not been resolved. The expression of MT1/2, but not of MT3 and MT4, in the liver and other mammalian organs can be induced by a variety of stimuli, including some trace metals (Cd, Hg, Zn, Ag, Pt), glucocorticoids, physical stress, inflammation, starvation, irradiation, chemicals that produce oxidative radicals, etc. [8-24]. From these studies various roles for MT1/2 have been proposed, such as intracellular storage and homeostatic control of essential metals (Zn, Cu), absorption and/or excretion of some essential and toxic metals, detoxication of toxic metals by sequestration, scavenging of free radicals, protection against alkylating agents, and resistance to and/or protection from anticancer drugs. Other studies indicated poorly-defined roles of MT1/2 and MT3 in regulation of mitochondrial energy metabolism in mammalian organs, protection from DNA damage and apoptosis, regulation of gene expression during certain stages of the cell cycle, cell proliferation and differentiation, organs development, transepithelial ion and water transport, cancerogenesis and cancer diagnostics, and pathogenesis of some neurodegenerative diseases [5,6,16,24-30]. MT3 has also been studied as a growth inhibitory factor (GIF) for neurons and glia in human brain [29,31].

In the mammalian kidneys, besides in homeostatic regulation of essential metals, MTs may play a protective role in nephrotoxicity induced by Cd and other toxic metals [11,16,32,33]. In adult rats, by biochemical and immunochemical methods a limited abundance of MT1/2 proteins was found largely in cortical proximal tubules [10,16,34-40], whereas the MT3 protein was detected in some glomerular and collecting duct cells [6]. In the human kidney, MT3 was demonstrated in the cytoplasm of epithelial cells in glomeruli, cortical proximal and distal tubules, and collecting ducts [4].

An independent, detailed immunolocalization of various MTs along the mammalian nephron has not been performed. A recent observation in MT3-transfected cell line of the human proximal tubule,

which exhibited formation of domes (not present in non-transfected cells), indicated that MT3 may be involved in the renal ion and water transport functions [5,41]. The MT3-transfected cells were also more sensitive to Cd-induced cytotoxicity [27,28]. These observations emphasized a need for a detailed characterization of MTs expression in various cell types along the mammalian nephron. In addition, a limited amount of MT1/2 has been detected in human and animal urine, but its origin has not been clarified; the urine MTs can be used as a biological marker of Cd exposure and Cd-induced renal dysfunctions [29,42-44]. In order to characterize the expression and localization of MTs in the rat kidneys, here we performed RT-PCR studies in various kidney zones of adult male rats, and immunochemical studies in tissue samples using the commercial (anti-MT1/2) and noncommercial (anti-MT3) antibodies. A possible expression of MT4 in the rat kidney was not a topic in this study, because previous mRNA studies indicated its absence in the mammalian kidneys [7,24].

2. Materials and methods

2.1. Animals, and human kidney

Male Wistar strain rats, 10-12 weeks old, from the breeding colony at the Institute for Medical Research and Occupational Health in Zagreb were used. Animals were bred and handled in accordance with the Directive 2010/63/EU on the protection of animals used for scientific purposes. Before and during experiments, animals had free access to standard laboratory food 4RF21 (Mucedola, Italy) and tap water.

Fresh tissue samples of human kidney cortex were obtained from the local hospitals in Zagreb. The samples were obtained from the adult male patiens that underwent surgical operations to remove tumors. Informed patient consent was obtained beforehand. The studies in rats and on human tissues were approved by the Institutional and hospital Ethic Committees.

2.2. Isolation of RNA, synthesis of first strand cDNA, and end-point RT-PCR

Rats were sacrificed under general anesthesia (Narketan, 80 mg/kg b.m. + Xylapan, 12 mg/kg b.m., i.p.; both from Chassot AG, Bern, Switzerland) by cutting large abdominal blood vessels and exsanguination under the stream of cold water. The kidneys were removed, decapsulated, rinsed in ice-

cold saline, and the middle, ~1 mm-thick transversal tissue slice was immediately immersed into RNAlater solution (Sigma, St. Louis, MO, USA). The slice was later separated in morphologically distinctive zones (cortex, outer stripe, inner stripe, and inner medulla (papilla)) for RNA isolation. Total cellular RNA from these tissue zones was extracted using Trizol (Invitrogen, Karlsruhe, Germany) and cleaned using the RNeasy Mini Kit (Qiagen, Hilden, Germany) according to manufacturer's instructions. RNA concentration and its purity was tested spectrophotometrically at 260 and 280 nm (BioSpec Nano, Shimadzu, Japan). The quality and integrity of RNA was further checked by agarose gel electrophoresis, stained with StarGel (Lonza, Rockland Inc., ME, USA), and visualized under ultraviolet light. Isolated RNA was stored at -70°C until use.

First strand cDNA synthesis was performed using the High Capacity cDNA RT Kit (Cat. #4374966; Applied Biosystems, Foster City, CA, USA) following the manufacturer's instructions. Total cellular RNA (1 μg) was incubated at 25°C for 10 min in the reaction mixture containing random primers and reverse transcribed in total volume of 50 μL containing 1x reverse transcription buffer, 20 units of ribonuclease inhibitor, 1 mM of dNTP mix, and 40 units of Multiscribe reverse transcriptase, by incubation at 37°C for 120 min and final denaturation at 85°C for 10 min. cDNAs were stored at -20°C until use..

RT-PCR was performed in total volume of 20 μL using: 1 μL of 5x diluted first strand cDNA, 0.4 μM specific primers, and ready to use PCR Master Mix (Applied Biosystems) following instructions by the manufacturer. To avoid amplification of genomic DNA, intron over-spanning primers were used. Custom primers for the rat genes, *rMT1* (subtype *MT1a*), *rMT2* (subtype *MT2A*), *rMT3*, and *rβ-actin* were purchased online from Invitrogen (http://bioinfo.ut.ee/primer3-0.4.0/). The primer sequences are listed in Table 1. Reaction conditions used for PCR were the following: initial denaturation for 3 min at 94°C, denaturation for 30 sec at 95°C, annealing for 30 sec at 57°C and elongation for 45 sec at 72°C. The non-template control, where the cDNA was substituted with DNase/RNase free water, exhibited no reaction (data not shown). RT-PCR products were resolved by electrophoresis in 1.5% agarose gel stained with 1xGelStar (Lonza, Rockland Inc., ME, USA), and visualized under ultraviolet light. The housekeeping gene *rβ-actin* was used to control variations in the

cDNA input. The optimal number of PCR cycles within the exponential phase of the reaction was 20 for *rMT1*, 24 for *rMT2* and *rβ-actin*, and 33 for *rMT3*.

2.3. Antibodies and other material

Commercial monoclonal anti-MT antibody (clone E9; Code M0639, generated against self-polymerized equine MT1 and MT2), which recognizes a highly conserved domain common to mammalian MT1 and MT2 proteins (MT1/2-ab), was purchased from DAKO (Carpinteria, CA, USA). This antibody was previously used to study MT1/2 in human organs [24] and in the organs of intact and Cd-treated rats [16,45], Noncommercial polyclonal antibody to human MT3/GIF (MT3-ab) was previously characterized in immunocytochemical and Western analysis in human organs and cell lines [4,5,27,28,41,46]. In this study we also used noncommercial polyclonal antibodies for water channels AQP1 (AQP1-ab; it stains the luminal and contraluminal membranes of proximal tubule and thin descending limb of Henle (TDLH), and blood capillaries [47]) and AQP2 (AQP2-ab; it stains the luminal membrane and intracellular vesicles of the collecting duct principal cells [48]), carboanhydrase II (CAII-ab; it stains the cytoplasm and nuclei of various cell types along the nephron with heterogeneous intensity [49]), carboanhydrase IV (CA IV-ab; it stains largely the apical membrane of S1 and S2 proximal tubule segments and thick ascending limb [50]), megalin (MEG-ab; it stains the brush-border membrane (BBM) and subapical endocytic vesiles in proximal tubules [51]), and thrombomodulin (TM-ab; it stains the endothelial cells in blood capillaries [52]). We also used the noncommercial rabbit-raised polyclonal antibody for 31-kDa subunit of vacuolar ATPase (V-ATPase-ab; it stains the proximal tubule subapical endosomes and other intracellular vacuoles [51]), noncommercial monoclonal antibody for Na^+/H^+-exchager 3 (NHE3-ab; it stains the proximal tubule BBM [51]), and commercial monoclonal antibody for α-tubulin (TUB-ab; it stains microtubules) [51,53]. FITC-phalloidin (BODIPY FL-Phallacidin, Molecular Probes, Eugene, OR) was used to stain actin filaments [53].

Secondary antibodies were the CY3-labeled donkey anti-mouse (DAMCY3) and goat anti-rabbit (GARCY3) IgG, FITC-labeled goat anti-mouse (GAMF) and goat anti-rabbit (GARF) IgG, and alkaline phosphatase-labeled goat anti-mouse (GAMAP) or goat anti-rabbit (GARAP) IgG. These antibodies were purchased from Jackson ImmunoResearch Laboratories, Inc. (West Grove, PA, USA)

or Kirkegaard and Perry (Gaithersburg, MD, USA), and were used in final concentration of 1.6 μg/ml (GARCY3), 2 μg/ml (DAMCY3), 8-10 μg/ml (GAMF and GARF), and 0.1 μg/ml (GAMAP and GARAP). Other chemicals in the study were the highest purity available and were purchased from either Sigma (St. Louis, MO, USA) or Fisher Scientific (New Jersey, NJ, USA).

2.4. Tissue fixation and immunocytochemistry

Under general anesthesia, the kidneys were perfused via the abdominal aorta, first with aerated (95% O_2/5% CO_2) and temperature-equilibrated (37°C) phosphate-buffered saline (PBS; in mM: 137 NaCl, 2.7 KCl, 1.8 KH_2PO_4, 10 Na_2HPO_4, pH 7.4) for ~2 min, and then with 50 ml PLP fixative (2% paraformaldehyde, 75 mM lysine, 10 mM sodium periodate) [54]. Kidneys were removed, sliced, and kept overnight in the same fixative at 4°C, followed by extensive washing in PBS, and storage in PBS containing 0.02% NaN_3 at 4°C until further use. Similarly, virtually healthy human kidney tissue was separated, rinsed in PBS, and immediately submerged in the fixative, left in it for ~24 h in a refrigerator, then extensively washed in PBS, and stored in PBS containing 0.02% NaN_3 at 4°C till cryosectioning.

To cut 4 μm frozen sections, tissue slices were infiltrated with 30% sucrose (in PBS) overnight, embedded in OCT medium (Tissue-Tek, Sakura, Japan), frozen at -25°C, and sectioned in a Leica CM 1850 cryostat (Leica instruments GmbH, Nussloch, Germany). Sections were collected on Superfrost/Plus Microscope slides (Fischer Scientific, Pittsburgh, PA; USA) and rehydrated in PBS for 10 min. Before applying the antibody, cryosections were pretreated for 5 min with 1% sodium dodecyl sulfate (1% SDS in PBS) in order to expose cryptic antigenic sites [55]. SDS was removed by extensive rinsing in PBS. Nonspecific binding of antibodies was prevented by incubating the sections with 1% bovine serum albumin (in PBS) for 15 min before applying primary antibodies.

In single-staining mode, cryosections were incubated in MT1/2-ab or MT3-ab (diluted in PBS 1:100) at 4°C overnight. This was followed by two washings in high salt PBS (PBS containing 2.7% NaCl) in order to decrease the nonspecific binding of antibodies plus two washings in regular PBS (5

min each). The sections were then incubated in secondary antibody DAMCY3 or GARCY3 for 60 min, and washed in PBS as above.

In double-staining mode, cryosections were first incubated in MT1/2-ab at room temperature (RT) overnight, followed by washings in PBS, then incubated at RT for 3 hours in optimal dilutions of polyclonal AQP1-ab, AQP2-ab, TM-ab (each 1:100), MEG-ab (1:1600), or CAII-ab (1:900), washed in PBS, then incubated in secondary antibodies DAMCY3 and GARF at RT for 60 min each, and washed in PBS. In other double-stainings, cryosections were incubated first in polyclonal V-ATPase-ab (1:100), MEG-ab (1:1600), or CAIV-ab (1:1000) at 4°C overnight, washed in PBS, incubated in monoclonal NHE3-ab (1:100) or TUB-ab (1:50) at RT for 3 hours, washed in PBS, followed by incubation in DAMCY3 and GARCY3 at RT for 60 min each, and washed in PBS. Alternatively, cryosections were incubated in CAII-ab (1:900) at 4°C overnight, washed in PBS, and then incubated in FITC-phalloidin (1:50) at RT for 15 min, and washed in PBS as above. After the last washing, cryosections were overlayed a fluorescence fading retardant without or with DAPI (Vectashield; Vector Laboratories Inc., Burlingame, CA, USA), coverslipped, and closed with nail polish.

Where needed, MT1/2-ab was blocked with the commercial equine kidney protein (final concentration 0.5 mg/ml; purchased from Sigma, St. Louis, MO, #M4766), whereas MT3-ab was blocked with the immunizing peptide (final concentration 0.2 mg/ml) at RT for 4 hours, and then used in immunostaining assay as described above.

The staining was examined with an Opton III RS fluorescence microscope (Opton Feintechnik, Oberkochen, Germany) and photographed using a Spot RT Slider camera and software (Diagnostic Instruments, Sterling Heights, MI, USA). The images were imported into Adobe Photoshop 6.0 for processing and labeling.

2.5. Preparation of tissue homogenates and isolation of cell cytosol and various organelles

Rats were sacrificed in deep anaesthesia by cutting abdominal blood vessels and exsanguination under the stream of cold water. Kidneys were removed, and tissue zones (cortex, outer stripe, inner stripe, inner medulla (papilla)) were dissected manually. The tissues were homogenized for one min in a chilled homo-buffer (in mM; 300 mannitol, 5 EGTA, 12 TRIS/HCl, pH 7.4, 1 phenyl-methyl-

sulfonyl-fluoride (PMSF), 0.1 benzamidine, and 0.1 μg/ml antipain) with a Powergen 125 homogenizer (Fisher Scientific, New Jersey, NJ, USA). To study MTs, tissue homogenates were centrifuged in a refrigerated high speed centrifuge (Sorvall RC-5C; rotor SS34) at 11,000 g for 30 min, the pellet was discarded, and the supernatant (denominated as homogenate) was further centrifuged at 19,000 g for 30 min. The obtained pellet was descarded, whereas the supernatant (denominated as tissue cytosol) was used for detection of MTs by immunoblotting. The pieces of fresh human kidney cortex were homogenized and processed the same way as described above for the rat tissue. The sample denominated as homogenate was used for Western blotting.

Preparations of BBM, basolateral membranes (BLM), and endocytic vesicles were isolated from the rat renal cortical homogenates by the established methods [56,57,58]. In accordance with our previous studies performed with the established enzyme activity assays [58,59], in 4 independent preparations, isolated BBM were enriched 15.9±1.65-fold and 1.4±0.3-fold in the activity of leucine arylamidase (EC 3.4.11.2) and Na^+/K^+-ATPase (EC 3.6.1.3), respectively. Isolated BLM were enriched 15.1±1.41-fold and 1.3±0.52-fold in the activity of Na^+/K^+-ATPase and leucine arylamidase, respectively, whereas isolated endocytic vesicles were enriched 38.5±1.72-fold, 2.4±0.17-fold and 0.52±0.16-fold in the activity of V-ATPase, alkaline phosphatase (EC 3.1.3.1) and Na^+/K^+-ATPase, respectively.

Nuclei from the rat kidney cortex homogenate were isolated by differential and sucrose density gradient centrifugation [60]. The images under phase-contrast indicated no significant contamination of isolated nuclei with other organelles. For immunocytochemical investigation, isolated nuclei were smeared on the plus slides, fixed with PLP fixative for 30 min, washed in PBS, and further processed for immunostaining with MT1/2-ab and MT3-ab, as described above for cryosections. In tissue homogenates and isolated organelles, protein was determined by the dye-binding assay [61], and the samples were stored at -20°C until further use.

2.6. SDS-PAGE and Western blotting

Before electrophoresis, tissue samples (homogenate, cytosol, isolated membranes, nuclei) were mixed with sample buffer (1% SDS, 12% v/v glycerol, 30 mM Tris/HCl, 5% β-mercaptoethanol, pH

6.8), and denatured at 95°C for 5 min. Proteins (10-50 μg protein per lane) were separated through 20% SDS-PAGE mini gels using the Vertical Gel Electrophoresis System and then electrophoretically wet-transferred using Mini Trans-Blot Electrophoretic Transfer Cell (both form Bio-Rad Laboratories, Hercules, CA, USA) to Immobilon membrane (Millipore, Bedford, MA, USA). Following transfer, the Immobilon membrane was incubated in 1% glutaraldehyde for 60 minutes to enhance MT retention in the membrane [62], washed several times with water and blocked in the blotting-buffer (5% nonfat dry milk, 0.15 M NaCl, 1% Triton-X-100, 20 mM Tris/HCl, pH 7.4) at RT for 60 min, followed by incubation in the same buffer that contained MT1/2-ab or MT3-ab (each 1:500 in PBS) at 4°C overnight. The membrane was then washed with several changes of blotting-buffer, incubated for 60 min in the same buffer that contained 0.1 μg/ml GAMAP or GARAP, washed again, and stained for alkaline phosphatase activity using the BCP/NBT (5-bromo-4chloro-3-indolyl phosphate/nitro blue tetrazolium) method to develop the antibody-related bands.

To test labeling specificity, MT1/2-ab and MT3-ab were blocked with the immunizing proteins (final concentration 0.5 mg/ml) at RT for 4 hours prior to the blotting assay. The labeled protein bands were evaluated by densitometry. The density of each band was scanned (Ultroscan Laser Densitometer, LKB, Bromma, Sweden), and the integrated scan surface was used in further calculations. In preliminary experiments we evaluated band densities with different amounts of protein and found that these parameters correlated well with up to 50 μg protein/lane (data not shown). The integrated surface of each scan was expressed in arbitrary units, relative to the surface of the densest band in the control samples (=100 arbitrary density units (DU)). In preliminary experiments, the optimal amounts of protein/gel lane, which gave linear relationship to the band density, were estimated and used in the following studies.

2.7. Transmission electron microscopy (TEM)

The PLP-fixed kidney cortex tissue was additionally fixed in 2% glutaraldehyde (in PBS) overnight and rinsed in PBS. The tissue was postfixed for 1 hour with 1% osmium tetroxid in cacodylated buffer. The material was dehydrated through an ethanol concentration series, embedded in

Spurr's medium, and ultrathin sections (70–80 nm) were cut with glass knife on an ultramicrotom RMC MT6000 XL (Sorvall, USA). The sections were mounted on Formvar-coated grids, stained with uranyl-acetat and lead-citrate, and viewed and photographed on transmission electron microscop Zeiss EM 10A (Carl Zeiss, Germany).

2.8. Processing of the data

The immunocytochemical and TEM figures represent findings in 3-4 rats. The images from both techniques were imported, assembled, and labeled in PhotoShop. The numeric data, expressed as means ± SEM, were evaluated by ANOVA/Duncan at 5% level of significance.

3. Results

3.1. Expression of MT1, MT2, and MT3 mRNA in tissue zones from male rat kidneys

As determined by end-point RT-PCR and estimated from the band size, the expression of *MT1* mRNA appeared strongest in the cortex, and much weaker and similar in other tissue zones (Fig. 1). The pattern of *MT2* mRNA expression was inner medulla>cortex>inner stripe>outer stripe, whereas the expression pattern of *MT3* mRNA was inner medulla>cortex=outer stripe=inner stripe. The localization and distribution of MT proteins along the nephron was further studied by immunochemical methods in tissue cryosections and isolated organelles using MT1/2-ab and MT3-ab.

3.2. Distribution of MT1/2 along the rat nephron

In cryosections of the kidney cortex, the MT1/2-ab-related immunostaining of variable intensity was detected in proximal convoluted tubules (Fig. 2A, and inset). The staining was largely cytoplasmic, at many places with clear bipolar appearance (inset), being intensive in the apical (large arrows) and basal (arrowheads) domains, but some tubule profiles remained partially or completely unstained. Some nuclei were also stained (thin arrows). In S3 segments of the outer stripe (Fig. 2B), the staining was more heterogeneous, being strong cytoplasmic (large arrows), weak cytoplasmic (large arrowheads), or absent (double small arrowheads), while nuclei were either weakly positive (thin arrows) or mostly unstained. Thick ascending limbs of Henle loop (TALH) in outer medulla exhibited

weak basal staining (Fig. 2C, arrows). However, some tubule profiles in the proximal region of inner medulla contained cells that were strongly stained in both cytoplasm and nuclei (Fig. 2D, arrows). In 4 rats, the immunoreactivity in this region was always present, however with heterogeneous intensity, from strong (Fig. 2D) to weak (not shown). More distal nephron parts, in the inner medulla (papilla) remained unstained (not shown).

In order to define the MT1/2-positive nephron segment in inner medulla, shown in Fig. 2D, cryosections of this region were double stained with MT1/2-ab and with antibodies for marker proteins known to be localized in the specific kidney structures. As shown in Fig. 3, the MT1/2-related staining did not colocalize with AQP1 in thin descending limbs and capillaries (A), with AQP2 in collecting ducts (B), and with thrombomodulin in capillaries (C). Therefore, we conclude that the nephron segment positive for MT1/2 was the thin ascending limb of Henle loop (thin ALH).

In order to further confirm the zonal-dependent abundance of MT1/2 protein, we performed Western blot analysis of the tissue homogenates (Fig. 4A and B) and isolated organelles (Fig. 4C). As shown in Fig. 4A, the broad MT1/2-ab-related protein band of 6-8 kDa was strongest in the cortex and weak in other tissue zones, in inner medulla being a slightly stronger than in the outer and inner stripe. The densitometric evaluation of these bands (Fig. 4B) confirmed the immunocytochemical pattern shown in Fig. 2. Furthermore, to test if the observed bipolar distribution of MT1/2-ab-related staining in the cortical proximal tubules, shown in Fig. 2A, was confined with specific cell organelles, the abundance of MT1/2 protein was tested by immunoblotting the tissue cytosol (TC) and isolated BBM, BLM, and endocytic vesicles (EV). As shown in Fig. 4C, the respective protein band was abundant in the tissue cytosol, but largely absent in isolated membrane organelles. A faint band of 7-8 kDa in isolated BBM may reflect a small content of MT1/2 protein encapsulated in membrane vesicles during homogenization.

3.3. MT1/2-rich organelles in the tubule lumen

In addition to intracellular staining, in the lumen of some cortical proximal tubule profiles we observed largely spheroid, droplet-like formations, brightly-stained with MT1/2-ab (Fig. 5A and B, arrows). These formations had various sizes (and, sometimes, different shapes), generally smaller than

the size of nucleus (<5 μm in diameter), and many of them were attached to the tubule BBM surface (Fig. 5B, arrow). The number of these formations per cryosection varied in different rats, from zero to a few, and their frequency in the female tubules was smaller than in males (not shown). This sex-related phenomenon was not further studied.

Serial images, double stained with MT1/2-ab and MEG-ab indicated that these luminal, MT1/2-rich formations may be generated by a developing process, which starts with budding of a small compartment from the apical cell domain and finishes with the final detachment (Fig. 5C-F, arrowheads). The cells that exhibited budding of MT1/2-rich droplets were usually stained strongly with MT1/2-ab, and had normal (non-fragmented) nucleus (Fig. 5G, arrows; as also indicated by the intact nuclei in TEM images (c.f. Fig. 7A)), excluding apoptosis as being involved. In the lumen of S3 segments, the usual MT1/2-rich formations were rare (Fig. 5H, arrowheads), mostly only the MT1/2-positive fragmented material was observed (Fig. 5H, arrows).

Double staining of these luminal formations with MT1/2-ab and several antibodies to cytoplasmic or membrane-bound antigens (Fig. 6A-G2) indicated that the MT1/2-rich formations are vesicles, surrounded by the NHE3-positive membrane (D1 and D2, arrows), which are strongly positive for CA II (A-C, arrows), but negative for V-ATPase (E1 and E2, arrows), actin (F1 and F2, arrows), tubulin (G1 and G2, arrows), and CA IV (not shown).

Budding of vesicles from the luminal cell domain in cortical proximal tubules, as a possible source of MT1/2-rich luminal vesicles was further indicated by TEM, where different stages of vesicle formation at the luminal cell surface can be observed (Fig. 7).

3.4. *Distribution of MT3 along the rat nephron*

The rabbit-raised antibody for C-terminal peptide of human MT3 was first tested for its staining efficiency in cryosections of the human kidney cortex, and by immunoblotting of the human kidney cortex homogenate (Fig. 8). As shown in Fig. 8A, MT3-ab stained with heterogeneous intensity the cell cytoplasm of proximal and distal tubules, and cortical collecting ducts. The staining was absent with the immunizing peptide-blocked MT3-ab (Fig. 8B). In Western blot of the cortex homogenate (Fig.

8C), MT3-ab labeled strongly the expected protein band of 7-8 kDa, and weakly a few upper bands (-P), all being absent with the peptide-blocked antibody (+P).

Immunoreactivity of MT3-ab in various tissue zones of the rat kidney is shown in Fig. 9. In various tubule profiles in the cortex (A and B), outer stripe (D), inner stripe (F), and inner medulla (H), the antibody stained the cell cytoplasm with heterogeneous, largely weak intensity, whereas nuclei in all renal structures were stronger stained (arrows). In some cortical proximal tubule profiles, a limited staining of BBM was also observed (A and B, arrowheads). The staining in all renal structures was absent with the peptide-blocked MT3-ab (C, E, G, I).

3.5. MTs in isolated renal nuclei

In order to test the presence of MT1/2 and MT3 in renal nuclei, nuclei from the rat kidney cortex were isolated by the established method, and probed by immunochemical methods with MT1/2-ab and MT3-ab (Fig. 10). Under phase contrast, the preparation of isolated nuclei appeared fairly devoid of other cellular structures as contaminats (Fig. 10A). By immunostaining, nuclei remained unstained with MT1/2-ab (Fig. 10B). On the contrary, the staining with MT3-ab was bright (Fig. 10C, and inset) and absent with the immunizing peptide-blocked antibody (Fig. 10D). In accordance with immunocytochemical data, in Western blots the isolated nuclei exhibited no MT1/2-ab-related protein band (Fig. 10E, N), whereas MT3-ab labeled the 7-8 kDa protein band (Fig. 10F, -Pept, N, arrow) and a few uper bands, all being absent or strongly diminished with the immunizing peptide-blocked antibody (Fig. 10F, +Pept, N).

4. Discussion

Using the methods of end-point RT-PCR in total cell RNA, indirect immunofluorescence cytochemistry in tissue cryosections, and Western blotting of variuos tissue samples, here we report on the expression and detailed immunolocalization of MT1/2 and MT3 in the kidneys of adult male rats. The RT-PCR data showed the presence of *MT1*, *MT2*, and *MT3* mRNA in all four tissue zones with heterogeneous expression; the expression of *MT1* mRNA was highest in the cortex, whereas the expression of *MT2* mRNA and *MT3* mRNA was highest in the inner stripe.

Immunolocalization of MT proteins was performed with commercial monoclonal MT1/2-ab and noncommercial polyclonal MT3-ab. Although the MT1/2-ab does not discriminate between MT1 and MT2 proteins, the pattern of mRNA expression indicates that the MT1 protein may be most abundant protein in the cortex, the MT2 protein may be most abundant in the inner medulla, whereas the MT3 protein may be distributed evenly in the cortex, outer stripe and inner stripe, and more abundant in the inner medulla. Heterogeneous, largely cytoplasmic but also nuclear immunoreactivity with MT1/2-ab was observed in several nephron segments, whereas in ascending thin limb, a weak immunoreactivity was exclusively cytoplasmic and located in the basal cell domain. Heterogeneity in the cytoplasmic content of MTs may be related to different, segment-specific metabolic rates that produce oxidative radicals, or to different exposure to toxic metals which are filtered via glomeruli, reabsorbed from the tubule lumen, and then acted by inducing synthesis of MTs [16]. Furthermore, being small molecules, MTs can be released from liver and other organs, filtered in glomeruli, and reabsorbed in proximal tubule by endocytosis [16]. However, the isolated renal cortical endocytic vesicles did not exhibit a visible protein band of MT1/2, indicating that in physiological conditions, filtration and endocytosis of the filtered MTs in male rats may be low, under detection limits. This phenomenon dramatically changes following treatment of rats with Cd or some other toxic metal, when the expression of MTs is strongly upregulated in hepatocytes and renal tubules, and MTs are released from both damaged hepatocytes and tubule cells [16], a condition also manifested with a detectable excretion of MT1/2 in urine [63].

In this study, the cytoplasmic MT1/2-ab-related staining in most cortical proximal tubules (S1/S2 segments) was distributed in two poles, stronger in the luminal and weaker in the contraluminal domain. In the outer stripe (S3 segments), however, the cytoplasmic staining was much weaker and homogeneous, without bipolar distribution. A predominant localization of MT1/2 staining in the luminal domain was previously reported in proximal tubules of the adult rat [38] and human kidneys [18], whereas in the study in human kidneys by Mididoddi et al. [24], the MT1/2 immunoreactivity was uniformly present in the proximal tubule cell cytoplasm. However, in this study we could not demonstrate a significant protein band of MT1/2 proteins in isolated luminal (BBM) and contraluminal

(BLM) membranes, indicating that the cytoplasmic proteins were not firmly associated with these membrane domains.

The cells with strongest abundance of MT1/2 immunoreactivity in the luminal domain seem to release a part of this cargo in form of vesicles, which were formed by exvagination of the BBM. The finding of MT1/2-positive material in the proximal tubule lumen of animal and human kidneys was previously described [21,34,35,38], but this phenomenon has not been further investigated. The fixation and staining techiques in our (PLP fixation *in vivo* and the indirect immunofluorescence staining in frozen tissue sections) and previous studies (Bouin's fixative or 10% buffered formalin by immersion and staining by immunoperoxidase method in paraffin sections) were different, thus indicating that the MT1/2-positive material in the tubule lumen was not related to the fixation and staining methods. Our studies with a single and double staining confirmed these findings as the MT1/2-positive vesicles in the lumen of cortical proximal tubules (S1/S2 segments), and further revealed that: a) MT1/2-rich vesicles seem to be formed by exvagination of the apical cell membrane (BBM) in the cells that are strongly stained for MT1/2 in their apical domain, in which various stages of the vesicle formation can be observed, b) the size of the MT1/2-rich vesicles is heterogeneous, 1-5 μm in diameter, and c) their limiting membrane was positive for the BBM marker NHE3, but not for megalin, V-ATPase and CA IV, whereas the intravesicular cargo contained the cytoplasmic MT1/2 and CA II, but not the cytoskeletal proteins actin and tubulin. However, we can not exclude the possibility that the vesicels contained all these proteins in very small concentrations, which were under the detection limits of our method.

The driving force for vesiculation of these MT1/2-rich formations and their detachment from the BBM is not clear. It may represent a process of continuous change in plasticity of the proximal tubule cells, where parts of BBM are removed by exvagination (shedding) in form of vesicles into the tubule lumen (a posibility shown also by TEM), and then replenished by newly synthetized membrane components *via* the intracellular vesicle trafficking. The observation that such vesicles are generated predominantly in the cells with very high subapical content of MT1/2 indicates that the apical accumulation of MTs in these cells may not be accidental, and may have some functional role in formation and detachment of the vesicles into the tubule lumen. The cells exhibiting formation of such

vesicles have intact nucleus, indicating that the observed vesiculation is not a part of apoptotic process. Rather, this phenomenon may be a physiologically-relevant secretory process to remove over-accumulated nontoxic and/or toxic cytoplasmic content in a bulk form.

The MT1/2-rich vesicles were relatively frequent in the lumen of proximal tubule S1/S2 segments in the cortex, rare and often fragmented in the lumen of proximal tubule S3 segments in the outer stripe, and absent in nephron segments located in more distal segments. The fragmented vesicles and liberated MTs may finish in urine, thus representing the source of MT1/2 in urine of intact, and much more in Cd-intoxicated animals and humans [42-44]. As suggested previously [16], the liberated MT1/2 in the tubule lumen may have a protective role by neutralizing ROS and RNS, and by binding toxic metals that may reach the tubule fluid by glomerular filtration or be released from the tubule cells. Also, these vesicles may be the source of various molecules for cell-to-cell communication (reviewed in [64]), CA II and other proteins (previously attributed to the glomerular filtration and "leakage" of the protein from the proximal and distal tubules [65]), and microvesicles and other membranous material in the urine of healthy people and of patients with kidney diseses [66].

As shown here, the cells in thin ascending limb of Henle represent another place of a significant immunoreactivity with MT1/2-ab, stronger in the nuclei than in the cytoplasm. The mRNA expression data in Fig. 1 suggest that the predominant MT isoform in this nephron segment may be MT2. Since the real function of individual MTs in mammalian cells is not known, a possible physiological rationale for predominant localization of MT2 in this part of the nephron remains to be determined in future studies.

Besides in the cytoplasm, a number of nuclei in the cells of proximal tubule S1, S2 and S3 segments also exhibited heterogeneous staining with MT1/2-ab. Similar heterogeneity in nuclear localization of MT1/2 was previously observed in the rat [19] and human [21,24] proximal tubules. However, the isolated nuclei from the renal cortex showed neither immunostaining nor protein band with MT1/2-ab, indicating that the MT1 and/or MT2 proteins were not firmly attached to the nuclear structures and were lost during isolation procedure. As reviewed before [16], the nuclear MT1/2 may originate from cytosol, but the exact mechanism of its translocation from the cytosol into the nucleus (and opposite) is not clear. The molecule is enough small to pass through the nuclear pores, but

possible triggers for this translocation and nuclear retention are unclear [67,68]. The nuclear MTs may deliver Zn and/or Cu needed for normal function of RNA, various metalloproteins (metalloenzymes, Zn-finger proteins), and growth and transcription factors that regulate the activity of various genes and protect the cell from ROS- and RNS-mediated DNA damage and apoptosis [69,70]. The high levels of MTs in nuclei indicate an increased need for Zn in metalloenzymes and transcription factors during rapid cell growth. Thus, the elevated nuclear presence of MTs in fetal period, in some cancers, and during liver regeneration after partial hepatectomy, indicates proliferative activity of the cells [25,71,72].

In contrast to *MT1* and *MT2* mRNA expression, the expression of *MT3* mRNA was relatively uniform in tissue zones, but slightly higher in inner medulla (papilla). Previous studies revealed a very heterogeneous expression of *MT3* mRNA and protein in various rat organs, highest in the brain, but very low in the heart, liver and kidneys. By immunocytochemistry in paraffin sections of the male rat kidneys, MT3 protein was previously detected in the cytoplasm of glomerular and collecting duct cells [6]. In human kidneys, the protein was demonstrated only in the cell cytoplasm of proximal and distal tubules, and collecting ducts [4]. These localizations are confirmed in the present immunocytochemical study in cryosections of the human kidney cortex. A number of previous studies showed that, different from MT1/2, whose expression was strongly upregulated by various inducers including Cd and Zn [16, and refrences in there], the *MT3* mRNA and protein expression was only transiently and weakly induced by these metals [3,73]. The studies in cultured human proximal tubule (HK-2) cells showed that the isoform MT3 may be involved in water and ion transport, contributing to domes formation [5], and may increase sensitivity of the cells to Cd-induced cytotoxicity, driving the mechanism of cell death from apoptosis to necrosis, possibly *via* activating early response genes *c-fos*, *c-jun* and *c-myc* [27,28,73]. The *MT3*-knockout mice were resistant to Cd-induced hepatotoxicity [15], thus indicating that this poory defined MT3-mediated mechanism of cytotoxicity operates also *in vivo* in some mammalian organs. In human brain cells, however, MT3 exhibited different roles; it showed neuroprotective function following traumatic or hypoxic brain damage, in cultured neurons acted as a growth inhibitory factor (GIF), while downregulation of its expression and loss of its protective and/or repair functions due to diminished cellular capacity to neutralize ROS may be

associated with Alzheimer's and other neurodegenerative diseases [31,74]. Furthermore, overexpression of *MT3* mRNA and/or related cytoplasmic protein was detected in many cases of human breast, bladder and prostatic cancers [75, and references in there].

As shown in the present study, the MT3-ab only weakly stained the cell cytoplasm of cortical proximal convoluted tubules, distal tubules and collecting ducts, and of S3 segments in the outer stripe. In some cortical proximal tubules, a weak staining of the luminal membrane was also observed. However, nuclei were heterogeneously stained in the cells of all nephron segments. The staning of granular appearance, and the respective protein band of 7-8 kDa in Western blot were retained in isolated cortical nuclei, indicating a firm association of MT3 with the unknown nuclear structures. The role of predominantly nuclear localization of MT3 protein in renal cells can be speculated in view of the known properties and functions of this and other metallothionenins. MT3 protein may primarily regulate intracellular concentration of Zn, where it exhibits some properties different from other MTs: a) it binds Zn ions more weakly, and exhibits higher metal-binding capacity than, for example, MT2, and b) binding to, and release of Zn from the molecule is a highly sensitive to redox state, which is related to production of ROS in oxidative stres [29,76, and references in there]. With these characteristics, MT3 may bring resistance to Zn toxicity in case of overloading, protect cells from ROS generated during normal and intense metabolism, and control Zn concentration in the cytoplasm and nuclei, necessary for optimal function of Zn-finger and other metalloproteins (enzymes, growth and transcription factors), which regulate activity of the genes, RNAs, and other cellular functions [69,70,76]. However, since MT3 Zn-binding sites are highly redox-sensitive, the protein can bind or release Zn in response to changes in oxidative status, and may even accelerate cell death due to cytotoxicity in acute oxidative injury caused by hyperproduction of ROS. In this condition, MT3 and other Zn-binding proteins release Zn ions which contribute to lysosomal membrane permeabilization and liberation of various catabolic enzymes, causing degradation of cellular content, cell necrosis and dead. On the other side, when cells are exposed to reducing conditions the apo-form of MT3 may bind more Zn. [76. and references in there].

5. Conclusion

Metallothioneins MT1, MT2, and MT3 are heterogeneously expressed in the cell cytoplasm and/or nuclei along the rat nephron. Some proximal tubule cells in the cortex exhibit very high abundance of MT1/2 in their apical domain. These cells may generate and release small, MT1/2-rich vesicles, which are detached from the luminal cell membrane and found in the tubule lumen. The vesicles may be formed by continuous change of the cell plasticity, which may be driven by intracellular MT1/2 by unknown mechanism, and may represent the source of urine MTs and vesicular material. In the tubule fluid, the intravesicular MT1/2 my protect the luminal membrane of tubular cells from the damaging effects of ROS- and/or NOS which may be filtered and/or released from the nephron cells. The MT3-related immunostaining was weak in the cell cytoplasm of various cortical tubules, and stronger in nuclei of all nephron segments. In these compartments, MT3 may regulate local concentration of Zn ions necessary for the function of various Zn-dependent proteins (enzymes, growth and transcription factors, Zn-finger proteins) that modulate the activity of genes, RNAs, and other cellular functions.

6. Acknowledgements and grants. The authors thank Mrs. Eva Heršak (deceased) and Ljiljana Babić for technical assistance, and Dr. Scott H. Garrett from Department of Pathology, School of Medicine and Health Sciences, University of North Dakota, Grand Forks, ND, USA, for generous donation of anti-MT3 antibody and the respective immunizing peptide. This work was supported partially by grant 022-0222148-2146 from Ministry for Science, Education and Sports, Republic of Croatia, and partially by grant IP-11-2013-1481 (AGEMETAR) from Croatian Science Foundation.

7. Disclosures. The authors declare no conflict of interest in this study.

8. Author contributions. M. Š., M. Lj., D. B., C. M. H-K., V.C., and N. Lj. performed experiments, prepared figures and tables, analyzed data, and drafted parts of manuscript. I.S. designed the concept of research, analyzed data, wrote the manuscript, and approved final version of the manuscript.

9. References

[1] P.F. Searle, B.L. Davidson, G. Stuart, T. Wilkie, G. Norstedt, R.D. Palmiter, Regulation linkage and sequence of mouse metallothionein I and II genes, Mol. Cell. Biol. 4 (1984) 1221-1230.

[2] R.D. Palmiter, S.D. Findley, T.E. Whitmore, D.M. Durnam, MT-III, a brain-specific member of the metallothionein gene family, Proc. Natl. Acad. Sci. USA 89 (1992) 6333-6337.

[3] J.G. Hoey, S.H. Garrett, M.A. Sens, J.H. Todd, D.A. Sens, Expression of MT-3 mRNA in human kidney, proximal tubule cell cultures, and renal cell carcinoma, Toxicol. Lett. 92 (1997) 149-160.

[4] S.H. Garrett, M.A. Sens, J.H. Todd, S. Somji, D.A. Sens, Expression of MT-3 protein in the human kidney, Toxicol. Lett. 105 (1999) 207–214.

[5] D. Kim, S.H. Garret, M.A. Sens, S. Somji, D.A. Sens, Metallothionein isoform 3 and proximal tubule vectorial active transport, Kidney Int. 61 (2002) 464-472.

[6] I. Hozumi, J.S. Suzuki, H. Kanazawa, A. Hara, M. Saio, T. Inuzuka, S. Miyairi, A. Naganuma, C. Tohyama, Metallothionein-3 is expressed in the brain and various peripheral organs of the rat, Neurosci. Lett. 438 (2008) 54-58.

[7] C. Quaife, S.D. Findley, J.C. Erickson, E.J. Kelly, P.B. Zambrowicz, R.D. Palmiter, Induction of a new metallothionein isoform (MT-IV) occurs during differentiation of stratified squamous epithelia, Biochemistry 33 (1994) 7250-7259.

[8] J.W. Bauman, J. Liu, Y.P. Liu, C.D. Klaassen, Increase in metallothionein produced by chemicals that induce oxidative stress, Toxicol. Appl. Pharmacol. 110 (1991) 347-354.

[9] I. Bremner, Nutritional and physiological significance of metallothioneins, Methods Enzymol. 205 (1991) 25-35.

[10] F.O. Brady, Induction of metallothionein in rats, Methods Enzymol. 205 (1991) 559-567.

[11] D.M. Templeton, M.G. Cherian, Toxicological significance of metallothionein, Methods Enzymol. 205 (1991) 11-23.

[12] M. Sato, I. Bremner, Oxygen free radicals and metallothionein, Free Rad. Biol. Med. 14 (1993.) 325-337.

[13] B.L. Vallee, The function of metallothionein, Neurochem. Int. 27 (1995) 23-33.

[14] P. Moffatt, C. Seguin, Expression of the gene encoding metallothionein-3 in organs of the reproductive system, DNA Cell Biol. 17 (1998) 501-510.

[15] A. Honda, H. Komuro, T. Hasegawa, Y. Seko, A. Shimada, H. Nagase, I. Hozumi, T. Inuzuka, H. Hara, Y. Fujiwara, M. Satoh, Resistance of metallothionein-III null mice to cadmium-induced acute hepatotoxicity, J. Toxicol. Sci. 35 (2010) 209-215.

[16] I. Sabolić, D. Breljak, M. Škarica, C.M. Herak-Kramberger, Role of metallothionein in cadmium traffic and toxicity in kidneys and other mammalian organs, Biometals 23 (2010) 897-926.

[17] K.L. Wong, C.D. Klaassen, Isolation and characterization of metallothionein which is highly concentrated in newborn rat liver, J. Biol. Chem. 254 (1979) 12399-12403.

[18] Y. Kojima, Y. Hamashima, Immunohistological studies of metallothionein II. Its detection in the human fetal kidney, Acta Histochem. Cytochem. 13 (1980) 277-286.

[19] M. Panemangalore, D. Banerjee, S. Onosaka, M.G. Cherian, Changes in the intracellular accumulation and distribution of metallothionein in rat liver and kidney during postnatal development, Dev. Biol. 97 (1983) 95-102.

[20] S.R. Clough, R.S. Mitra, A.P. Kulkami, Qualitative and quantitative aspects of human fetal liver metallothioneins, Biol. Neonate 49 (1986) 241-254.

[21] N.O. Nartey, D. Banerjee, M.G. Cherian, Immunohistochemical localization of metallothionein in cell nucleus and cytoplasm of fetal human liver and kidney and its changes during development, Pathology 19 (1987) 233-238.

[22] H.M. Chan, M.G. Cherian, Ontogenic changes in hepatic metallothionein isoforms in prenatal and newborn rats. Biochem. Cell Biol. 71 (1993) 133-140.

[23] M.G. Cherian, Nuclear and cytoplasmic localization of metallothionein in human liver during development and in tumor cells. In K.T. Suzuki, N. Imura and M. Kimura (Eds.), Metallothionein III, Birkhauser Verlag, Basel, 1993, pp. 175-187.

[24] S. Mididoddi, J.P. McGuirt, M.A. Sens, J.H. Todd, D.A. Sens, Isoform-specific expression of metallothionein mRNA in the developing and adult human kidney, Toxicol. Lett. 85 (1996) 17-27.
[25] M.G. Cherian, M.D. Apostolova, Nuclear localization of metallothionein during cell proliferation and differentiation, Cell. Mol. Biol. 46 (2000) 347-356.
[26] B. Ye, W. Maret, B.L. Vallee, Zinc metallothionein imported into liver mitochondria modulates respiration, Proc. Natl. Acad. Sci. USA 98 (2001) 2317-2322.
[27] S. Somji, S.H. Garrett, M.A. Sens, V. Gurel, D.A. Sens, Expression of metallothionein isoform 3 (MT-3) determines the choice between apoptotic or necrotic cell death in Cd^{+2}-exposed human proximal tubule cells, Toxicol. Sci. 80 (2004) 358–366.
[28] S. Somji, S.H. Garrett, M.A. Sens, D.A. Sens, The unique n-terminal sequence of metallothionein-3 is required to regulate the choice between apoptotic or necrotic cell death of human proximal tubule cells exposed to Cd^{+2}, Toxicol. Sci. 90 (2006) 369–376.
[29] E. Carpene, G. Andreani, G. Isani, Metallothionein functions and structural characteristics, J. Trace Elem. Med. Biol. 21 (2007) 35-39.
[30] J. Gumulec, M. Raudenska, V. Adam, R. Kizek, M. Masarik, Metallothionein – immunohistochemical cancer biomarker: A meta-analysis, PLOS ONE 9 (e85346), (2014) 1-14.
[31] S. Tsuji, H. Kobayashi, Y. Uchida, Y. Ihara, T. Miyatake, Molecular cloning of human growth inhibitory factor cDNA and its down-regulation in Alzheimer's disease, EMBO J. 11 (1992) 4843-4850.
[32] Y.P. Liu, J. Liu, S.M. Habeebu, C.D. Klaassen, Metallothionein protects against the nephrotoxicity produced by chronic CdMT, Toxicol. Sci. 50 (1999) 221-227.
[33] Y. Liu, J. Liu, S.M. Habeebu, M.P. Waalkes, C.D. Klaassen, Metallothionein-I/II null mice are sensitive to chronic oral cadmium-induced nephrotoxicity, Toxicol. Sci. 57 (2000) 167-176.
[34] K.G. Danielson, S. Ohi, P.C. Huang, Immunochemical detection of metallothionein in specific epithelial cells of rat organs, Proc. Natl. Acad. Sci. USA 79 (1982) 2301-2304.
[35] K.G. Danielson, S. Ohi, P.C. Huang, Immunochemical localization of metallothionein in rat liver and kidney, J. Histochem. Cytochem. 30 (1982) 1033-1039.
[36] R.E. Dudley, L.M. Gammal, C.D. Klaassen, Cadmium-induced hepatic and renal injury in chronically exposed rats: likely role of hepatic cadmium-metallothionein in nephrotoxicity, Toxicol. Appl. Pharmacol. 77 (1985) 414-426.
[37] M.P. Waalkes, C.D. Klaassen, Concentration of metallothionein in major organs of rats after administration of various metals, Toxicol. Sci. 5 (1985) 473-477.
[38] C. Tohyama, H. Nishimura, N. Nishimura, Immunohistochemical localization of metallothionein in the liver and kidney of cadmium- or zinc-treated rats. Acta Histochem. Cytochem. 21 (1988) 91-102.
[39] A. Tanimoto, T. Hamada, K. Higashi, Y. Sasaguri, Distribution of cadmium and metallothionein in $CdCl_2$-exposed rat kidney: Relationship with apoptosis and regeneration, Pathol. Int. 49 (1999) 125-132.
[40] M. Kuwahara, T. Ota, Y. Gu, T. Asai, Y. Terada, T. Akiba, F. Marumo, Renal expression of metallothionein in rats treated with cadmium. Clin. Exp. Nephrol. 6 (2002) 79-84.
[41] A. Slusser, C.S. Bathula, D.A. Sens, S. Somji, M.A. Sens, X.D. Zhou, S.H. Garrett, Cadherin expression, vectorial active transport, and metallothionein isoform 3 mediated EMT/MET responses in cultured primary and immortalized human proximal tubule cells, PLOS ONE 24 (2015) 1-28.
[42] C. Tohyama, Z.A. Shaikh, K.J. Ellis, S.H. Cohn, Metallothionein excretion in urine upon cadmium exposure: Its relationship with liver and kidney cadmium, Toxicology 22 (1981) 181-191.
[43] C. Tohyama, Z.A. Shaikh, Metallothionein in plasma and urine of cadmium-exposed rats determined by a single-antibody radioimmunoassay, Fundam. Appl. Toxicol. 1 (1981) 1-7.
[44] Z.A. Shaikh, T. Kido, H. Kito, R. Honda, K. Nogawa, Prevalence of metallothioneinuria among the population living in the Kakehashi River basin in Japan – an epidemiological study, Toxicology 64 (1990) 59-69.

[45] I. Sabolić, C.M. Herak-Kramberger, D. Brown, Subchronic cadmium treatment affects the abundance and arrangement of cytoskeletal proteins in rat renal proximal tubule cells, Toxicology 165 (2001) 205–216.
[46] A. Slusser, Y. Zheng, X.D. Zhou, S. Somji, D.A. Sens, M.A. Sens, S.H. Garrett, Metallothionein isoform 3 expression in human skin, related cancers and human skin derived cell cultures, Toxicol. Lett. 232 (2015) 141–148.
[47] I. Sabolić, G. Valenti, J-M. Verbavatz, A.N. Van Hoek, A.S. Verkman, D.A. Ausiello, D. Brown, Localization of the CHIP28 water channel in rat kidney, Am. J. Physiol. Cell Physiol. 263 (1992) C1225-C1233.
[48] I. Sabolić, T. Katsura, J-M. Verbavatz, D. Brown, The AQP2 water channel: effect of vasopressin treatment, microtubule disruption, and distribution in neonatal rats, J. Membr. Biol. 143 (1994) 165-175.
[49] D. Brown, T. Kumpulainen, J. Roth, L. Orci, Immunohistochemical localization of carbonic anhydrase in postnatal and adult rat kidney, Am. J. Physiol. Renal Physiol. 245 (1983) F110-F118.
[50] D. Brown, X.L. Zhu, W.S. Sly, Localization of membrane-associated carbonic anhydrase type IV in kidney epithelial cells, Proc. Natl. Acad. Sci. USA 87 (1990) 7457-7461.
[51] I. Sabolić, M. Ljubojević, C.M. Herak-Kramberger, D. Brown, Cd-MT causes endocytosis of brush-border ransporters in rat renal proximal tubules, Am. J. Physiol. Renal Physiol. 283 (2002) F1389-F1402.
[52] I. Sabolić, O. Čulić, S-H. Lin, D. Brown, Localization of ecto-ATPase in rat kidney and isolated renal cortical membrane vesicles, Am. J. Physiol. Renal Physiol. 262 (1992) F217-F228.
[53] V. Crljen, I. Sabolić, J. Sušac, D. Appenroth, C.M. Herak-Kramberger, M. Ljubojević, N. Anzai, R. Antolović, G. Burckhardt, C. Fleck, I. Sabolić, Immunocytochemical characterization of the incubated rat renal cortical slices, Pflügers Arch. Eur. J. Physiol. 450 (2005) 269-279.
[54] I.W. McLean, P.F. Nakane, Periodate-lysine paraformaldehyde fixative: a new fixative for immunoelectron microscopy, J. Histochem. Cytochem. 22 (1974) 1077-1083.
[55] D. Brown, J. Lydon, M. McLaughlin, A. Stuart-Tilley, R. Tyszkowski, S. Alper, Antigen retrieval in cryostat tissue sections and cultured cells by treatment with sodium dodecyl sulfate (SDS). Histochem. Cell Biol. 105 (1996) 261-267.
[56] J. Biber, B. Steiger, W. Haase, H. Murer, A high yield preparation for rat kidney brush border membranes. Different behaviour of lysosomal markers, Biochem. Biophys. Acta 647 (1981) 169-176.
[57] V. Scalera, Y.K. Huang, B. Hildmann, H. Murer, A simple isolation method for basal-lateral plasma membranes from rat kidney cortex, Membrane Biochem. 4 (1981) 49-64.
[58] I. Sabolić, G. Burckhardt, ATP-driven proton transport in vesicles from rat kidney cortex, Methods Enzymol. 191 (1990) 505-520.
[59] I. Sabolić, G. Burckhardt, Proton pathways in rat renal brush-border and basolateral membranes, Biochim. Biophys. Acta 734 (1983) 210-220.
[60] G. Blobel, V.R. Potter, Nuclei from rat liver: isolation method that combines purity with high yield, Science 154 (1966) 1662-1665.
[61] M.M. Bradford, A rapid and sensitive method for the quantitation of microgram quantities of protein utilizing the principle of protein-dye binding, Anal. Biochem. 72 (1976) 248-254.
[62] C.A. Mizzen, N.J. Cartel, W.H. Yu, P.E. Fraser, D.R. McLachlan, Sensitive detection of metallothioneins-1, -2 and –3 in tissue homogenates by immunoblotting: a method for enhanced membrane transfer and retention, J. Biochem. Biophys. Methods 32 (1996) 77-83.
[63] N. Sugihira, C. Tohyama, M. Marukami, H. Saito, Significance of increase in urinary metallothionein of rats repeatedly exposed to cadmium, Toxicology 41 (1986) 1-9.
[64] G. Turturici, R. Tinnirello, G. Sconzo, F. Geraci, Extracellular membrane vesicles as a mechanism of cell-to-cell communication: advantages and disadvantages, Am. J. Physiol. Cell Physiol. 306 (2014) C621-C633.
[65] U. Backman, B. Danielsson, P.J. Wistrand, The excretion of carbonic anhydrase isoenzymes CA I and CA II in the urine of apparently healthy subjects and in patients with kidney disease, Scand. J. Clin. Lab. Invest. 50 (1990) 627-633.

[66] M. Knepper, T. Pisitkun, Exosomes in urine: Who would have thought…?, Kidney Int. 72 (2007) 1043-1045.
[67] M. Levadoux, C. Mahon, J.H. Beattie, H.M. Wallace, J.E. Hesketh, Nuclear import of metallothionein requires its mRNA to be associated with the perinuclear cytoskeleton, J. Biol. Chem. 274 (1999) 34961–34966.
[68] Y. Takahashi, Y. Ogra, K.T. Suzuki, Nuclear trafficking of metallothionein requires oxidation of a cytosolic partner, J. Cell. Physiol. 202 (2005) 563–569.
[69] Y. Ogra, K.T. Suzuki, Nuclear trafficking of metallothionein. Possible mechanisms and current knowledge, Cell. Mol. Biol. 46 (2000) 357–365.
[70] D.H. Petering, S. Krezoski, N.M. Tabatabai, Metallothionein toxicology: metal ion trafficking and cellular protection, Met. Ions Life Sci. 5 (2009) 353–397.
[71] C. Tohyama, J.S. Suzuki, J. Hemelraad, N. Nishimura, H. Nishimura, Induction of metallothionein and its localization in the nucleus of rat hepatocytes after partial hepatectomy, Hepatology 18 (1993) 1193-1201.
[72] M.G. Cherian, The significance of the nuclear and cytoplasmic localization of metallothionein in human liver and tumor cells, Environ. Health. Perspect. 102 (Suppl 3) (1994) 131-135.
[73] S.H. Garrett, V. Phillips, S. Somji, M.A. Sens, R. Dutta, S. Park, D. Kim, D.A. Sens, Transient induction of metallothionein isoform 3 (MT-3), *c-fos*, *c-jun* and *c-myc* in human proximal tubule cells exposed to cadmium, Toxicol. Lett. 126 (2002) 69–80.
[74] W.H. Yu , W.J. Lukiw, C. Bergeron, H.B. Niznik, P.E. Frase, Metallothionein III is reduced in Alzheimer's disease, Brain Res. 894 (2001) 37–45.
[75] M.A. Sens, S. Somji, S.H. Garrett, C.L. Beall, D.A. Sens, Metallothionein isoform 3 overexpression is associated with breast cancers having a poor prognosis, Am. J. Pathol. 159 (2001) 21-26.
[76] S-J. Lee, J-Y. Koh, Roles of zinc and metallothionein-3 in oxidative stress-induced lysosomal dysfunction, cell death, and autophagy in neurons and astrocytes, Mol. Brain 3 (2010) 30, doi:10.1186/1756-6606-3-30.

Table 1. Primer sequences used in end-point RT-PCR studies of rat metallothionein genes

Gene	Forward (F)/Reverse (R) Primers (5'-3')	Accession No. Gene Bank	Location	RT-PCR product (bp)
rMT1a	F: CACCAGATCTCGGAATGGAC	NM_138826.4	56-75	220
	R: CAGCAGCACTGTTCGTCACT		275-256	
rMT2A	F: CACAGATGGATCCTGCTCCT	NM_001137564.1	86-105	249
	R: AAGTGTGGAGAACCGGTCAG		334-315	
rMT3	F: CCTGGATATGGACCCTGAGA	NM_053968.2	60-80	249
	R: AGGGACACGCAGCACTATTC		308-288	
rβ-Actin	F: GTCGTACCACTGGCATTGTG	NM_031144.2	518-537	364
	R: AGGAAGGAAGGCTGGAAGAG		862-881	

10. Figure legends

Fig. 1. Expression of *MTs* mRNA as determined by end-point RT-PCR in kidney tissue zones of an adult male rat. A housekeeping gene *β-actin* is similarly expressed in all tissue zones. The data are representative for similar findings in 3 rats. CO, cortex; OS, outer stripe; IS, inner stripe; IM, inner medulla (papilla.

Fig. 2. Immunolocalization of MT1/2 along the nephron of an adult male rat. **A. Cortex** (and inset). In proximal convoluted tubules, the MT1/2-ab-related immunostaining was heterogeneous in intensity, and in many places with bipolar appearance, being concentrated in subapical (thick arrows) and basal (arrowheads) domains of the tubule epithelium. Some nuclei were aslo clearly stained (thin arrows). Glomeruli and other nephron segments in the cortex remained unstained (not shown). **B. Outer stripe**. Heterogeneous staining in the cells of S3 segments; the staining was strong (thick arrows) or weak (large arrowheads) cytoplasmic, or absent (small double arrowheads). Most nuclei were unstained, but some nuclei were clearly stained (thin arrows). **C. Inner stripe**. Thick ascending limbs of Henle exhibited weak staining at the basal domain (arrows). **D. Inner medulla**. Thin tubule profiles in the proximal region of inner medulla contained cells that expressed high levels of the staining in both cytoplasm and nuclei (arrows). More distal nephron parts in the inner medulla (papilla) remained unstained (not shown). Bar, 20 μm.

Fig. 3. Characterization of MT1/2-positive nephron segment in inner medulla; double staining using antibodies for specific marker proteins. **A.** Staining with MT1/2-ab (red fluorescence, arrowheads) and AQP1-ab (green fluorescence) did not colocalize; AQP1 was localized in the plasma membrane of descending thin limb of Henle (large arrows) and blood capillaries (thin double arrows). **B.** Staining with MT1/2-ab (red fluorescence, large arrowheads) and AQP2-ab (green fluorescence, large arrows) did not colocalize; AQP2 was localized in the principal cells of inner medullary collecting duct. Dark cells in the collecting ducts remained unstained with both antibodies (thin double arrows). **C**. Staining

with MT1/2-ab (red fluorescence, arrowheads) and TM-ab (green fluorescence) did not colocalize; thrombomodulin was localized in blood capillaries (arrows). Bar (for all images), 20 μm.

Fig. 4. Western blot of MT1/2 in tissue cytosol and isolated organelles from various zones of the rat kidney. **A.** The abundance of MT1/2 in tissue cytosol from the kidney cortex (CO), outer stripe (OS), inner stripe (IS), and inner medulla (IM) of male rats. Each protein band represents a tissue sample (50 μg protein/lane) from separate animal. **B**. Densitometric evaluation of the bands shown in A. Each bar is the mean ± SEM of the data in tissue cytosols from 3-4 rats. Statistics (ANOVA): a vs. b, c or d, $P < 0.001$; c vs. d, $P < 0.05$. Other relations, not significant. DU = arbitrary density units. **C.** Abundance of MT1/2 in tissue cytosol (TC) and in brush-border membranes (BBM), basolateral membranes (BLM), and endocytic vesicles (EV) isolated from the kidney cortex. Each band represents protein sample (50 μg protein/lane) from separate animal.

Fig. 5. Immunolocalization of MT1/2-rich spherical formations (organelles) in the lumen of proximal tubules. **A-B**, MT1/2-rich formations in the lumen of some cortical proximal tubules (arows). **C-F**, Serial images indicating formation, budding, and detachment of MT1/2-rich organelle (arrowheads) *via* an apical process from the MT1/2-rich epithelial cells. Double staining with MT1/2-ab (red fluorescence) and MEG-ab (green fluorescence). The final, detached organelles (F, arrowheads) were strongly positive for MT1/2 and negative for MEG. **G**. Double staining of proximal tubule with MT1/2-ab (red fluorescence) and nuclei with DAPI (blue fluorescence). The cells that form and shed MT1/2-rich organells (arrowheads) had normally-shaped nuclei (arrows). **H**. Double staining with MT1/2-ab (red fluorescence) and MEG-ab (green fluorescence) in cryosections of outer stripe. In the lumen of S3 segments, the compact MT1/2-rich organelles were rare (arrowheads) and largely fragmented (arrows). In more distal parts of the nephron, these organelles were not observed (not shown). Bars, 20 μm.

Fig. 6. Immunocytochemical characterization of MT1/2-rich organelles in the proximal tubule lumen; double staining with using antibodies for specific proteins. **A-C**, Immunostaining with MT1/2-ab (A, red staining, arrows), CA2-ab (B, green staining, arrows), and merged image (C, arrows) showed a complete colocalization, giving brightly yellow-stained organelles. **D1-D2**, CA2-positive organelle (D1, green staining, arrow) was surrounded with the NHE3-ab-positive membrane (D2, red staining, arrow), proving the MT1/2-rich formation being a vesicle. NHE3-ab also stained strongly the tubule BBM (D2, arrowhead). The general intensity of red fluorescence was enhanced in PhotoShop in order to reveal weak staining of the vesicle limiting membrane. **E1-E2,** The MT1/2-rich vesicle (E1, green stained, arrow) was co-stained with V-ATPase-ab (E2, red fluorescence, arrow). V-ATPase-ab stained subapical endocytic vesicles (E2, arrowhead) and intracellular vacuoles (mainly lysosomes), but not the MT1/2-rich vesicle (E2, arrow). **F1-F2,** MT1/2-rich vesicle (F1, red staining, arrow) was co-stained with FITC-phalloidin, a marker for actin in BBM (F2, green, arrowhead). The MT1/2-rich vesicle was negative for actin (F2, arrow). **G1-G2,** the CA2-positive vesicle in the tubule lumen (G1, green staining, arrow) was not stained with TUB-ab (G2, arrow), wich stained microtubules in the tubule epithelial cells (G2, red staining, arrowhead). Similarly, the MT1/2-rich vesicles were not stained with CA4-ab (data not shown). Bar, 20 μm for all images.

Fig. 7. Transmission electron microscopy of the cortical proximal tubule from the adult male rat kidney; possible source of putative MT1/2-rich organelles in the tubule lumen. Shown are various stages of formation by budding and shedding of membrane vesicles (asterisks) that may contain MT1/2 and other cytoplasmic molecules. **A,** The would-be vesicle with a wide connection to the cell surface. **B,** The vesicle with a thin connection to the cell surface. **C,** Fully detached vesicle. **D,** Free, round-shape vesicles of heterogeneous size in the tubule lumen. The limiting vesicle membrane is indicated by strong contrast (arrowheads). BB, brush border microvilli. N, nucleus. Bars, 1.5 μm.

Fig. 8. Immunoreactivity of MT3-ab in the human kidney cortex tissue. **A,** The cell cytoplasm of proximal (PT) and distal (asterisk) tubules, and of cortical collecting duct (CD) were stained with heterogeneous intensity. The cells in glomerulus (G) and nuclei in the tubule epithelium remained

unstained. **B,** Absence of staining with the immunizing peptide-blocked MT3-ab. **C,** Western blot of the cortex homogenate with MT3-ab. Labeled was strongly the protein band of 7-8 kDa, and weakly a few upper bands, probably reflecting polymerized proteins (-P). All the bands were abolished with the immunizing peptide-blocked antibody (+P).

Fig. 9. Immunoreactivity of MT3-ab in various kidney zones of the adult male rat (**A, B, D, F, H**) and its absence with the immunizing peptide-blocked antibody (**C, E, G, I**). In the cells of glomeruli and various tubule profiles in the cortex (**A** and **B**), outer stripe (**D**), inner stripe (**F**), and inner medulla (**H**), cytoplasm was heterogeneously but weakly stained, whereas nuclei in all renal structures were stronger stained (arrows). Some cortical proximal tubules also exhibited variable staining of the luminal membrane (A and B, arrowheads). The staining in all structures was absent with the peptide-blocked MT3-ab (C, E, G, I). G, glomeruli; S1 and S3, proximal tubule S1 and S3 segments; DT, distal tubule; CD, collecting duct; TALH, thick ascending limb of Henle loop. Bar, 20 μm for all images.

Fig. 10. MT1/2 and MT3 in isolated nuclei; immunocytochemical (**A-D**) and Western blot studies (**E** and **F**). **A** (and inset), Dark field image of nuclei isolated from the kidney cortex. **B,** Absence of immunoreactivity with MT1/2 antibody in isolated nuclei. **C** (and inset), strong immunoreactivity with MT3-ab in isolated nuclei. **D,** Absence of immunoreactivity with the peptide-blocked MT3-ab. Bar, 20 μm for all immages. **E,** Western blot of the renal cortical homogenate (HOM) and isolated nuclei (N) with MT1/2-ab. **F,** Western blot of the renal cortical homogenate (HOM) and isolated nuclei (N) with MT3-ab (-Pept) and with the peptide-blocked MT3-ab (+Pept). 7-8 kDa protein band, labeled with MT3-ab is indicated with an arrow. Each lane contained 50 μg protein.

Fig. 1

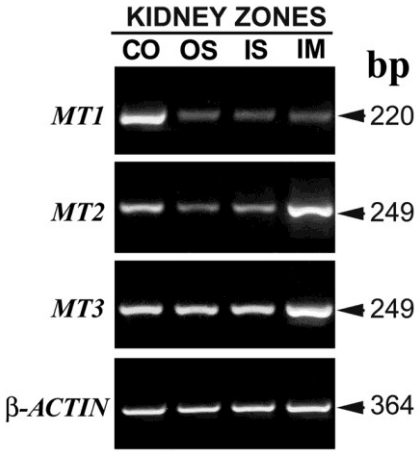
KIDNEY ZONES
CO OS IS IM
bp
MT1
220
MT2
249
MT3
249
β-ACTIN
364

Fig. 2.

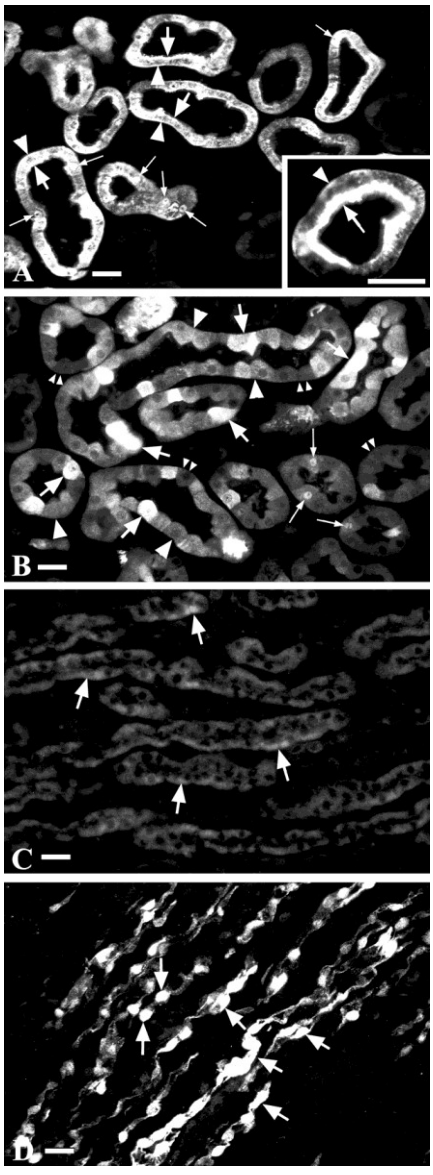
A
B
C
D

Fig. 3.

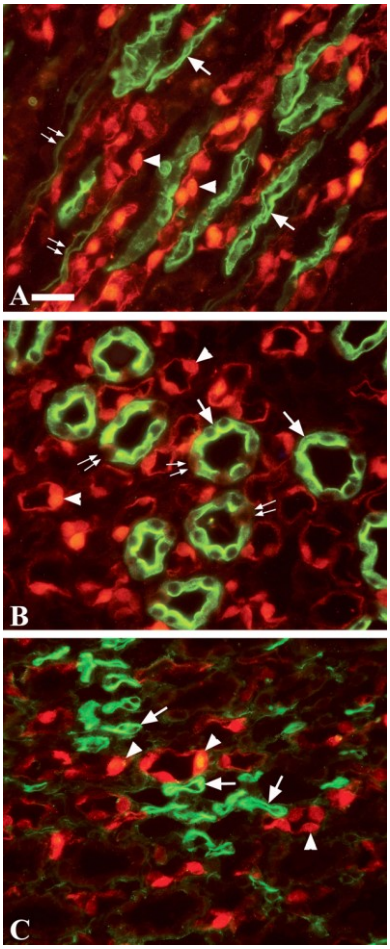
A
B
C

Fig. 4.

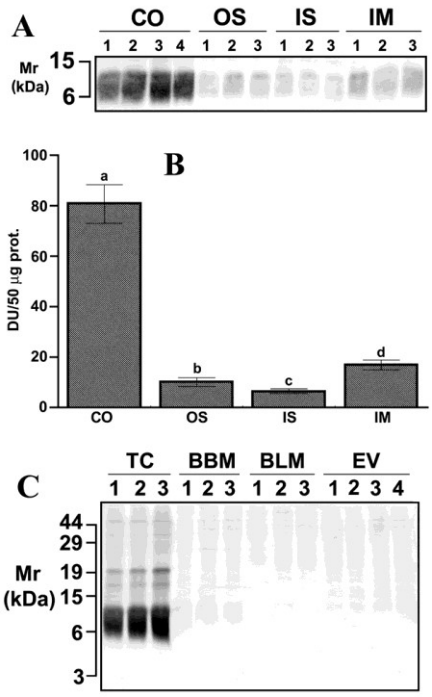
A
CO
OS
IS
IM
1 2 3 4 1 2 3 1 2 3 1 2 3
Mr (kDa)
15
6
B
DU/50 µg prot.
100
80
60
40
20
0
a
b
c
d
CO
OS
IS
IM
C
TC
BBM
BLM
EV
1 2 3 1 2 3 1 2 3 1 2 3 4
44
29
19
15
6
3
Mr (kDa)

Fig. 5.

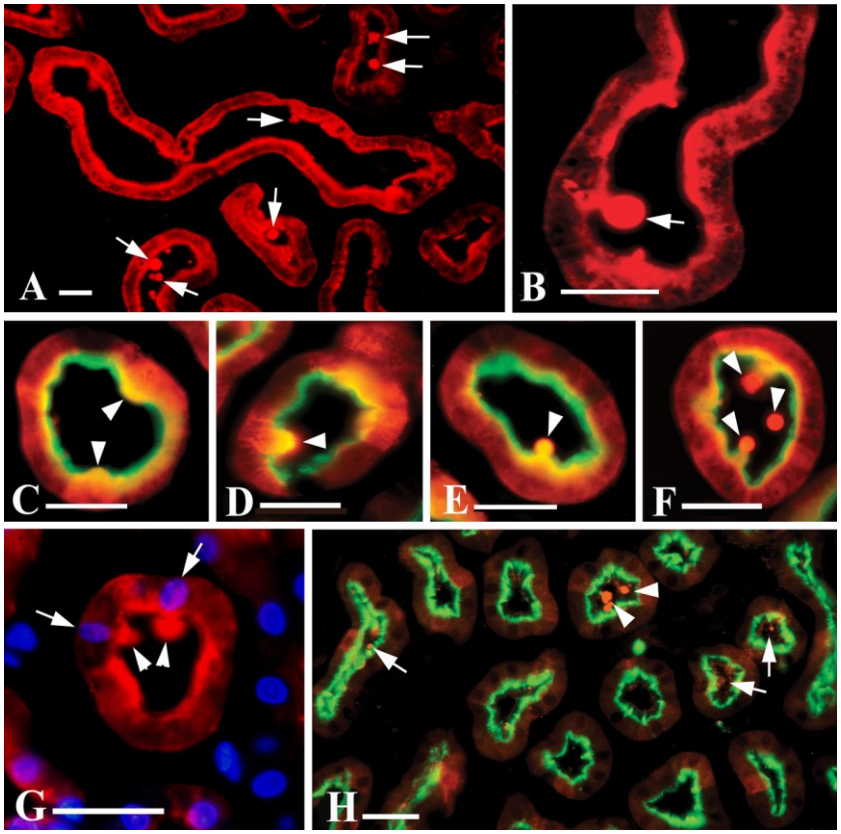

Fig. 6.

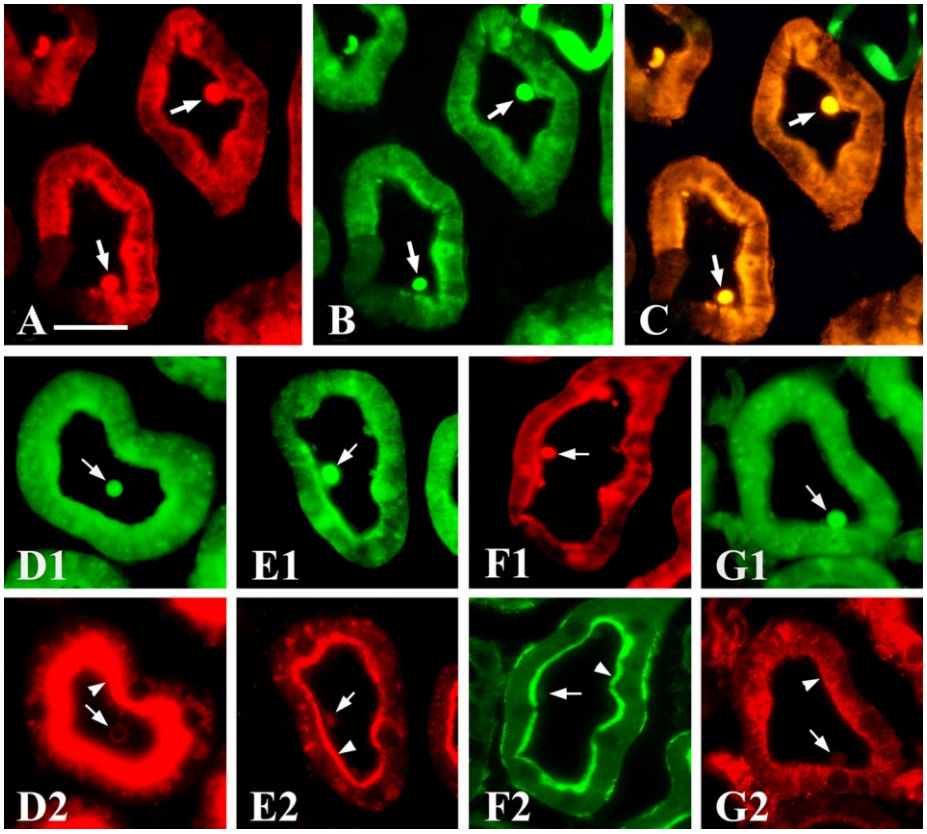

Fig. 7.

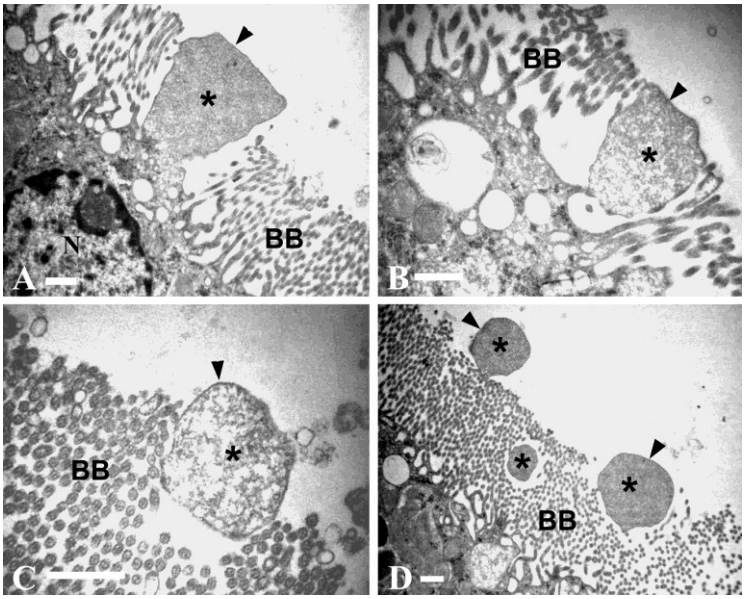

Fig. 8.

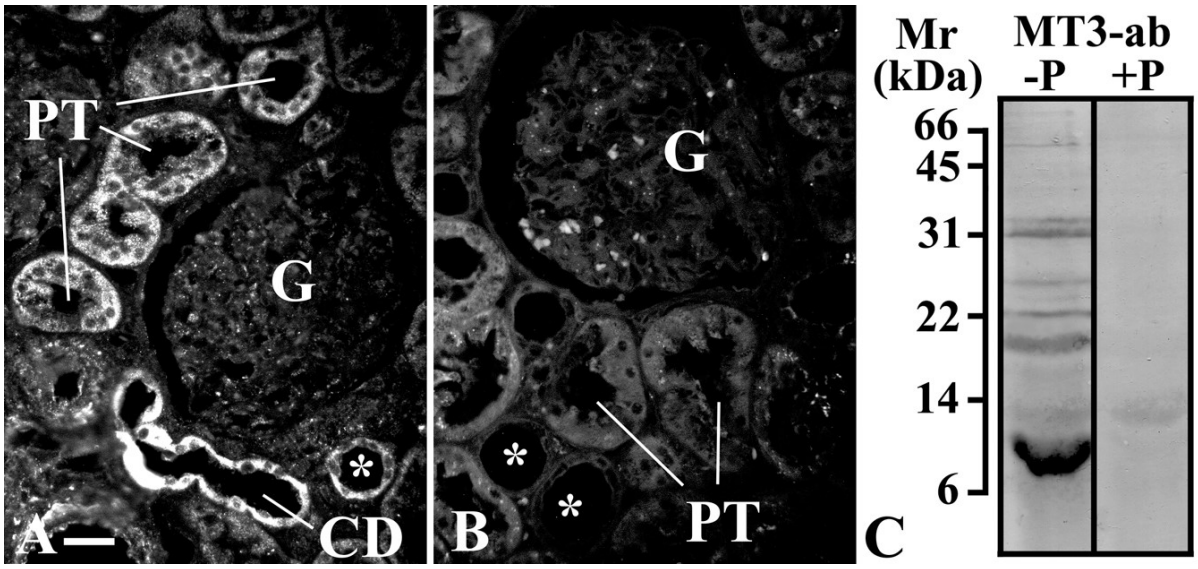

Fig. 9.

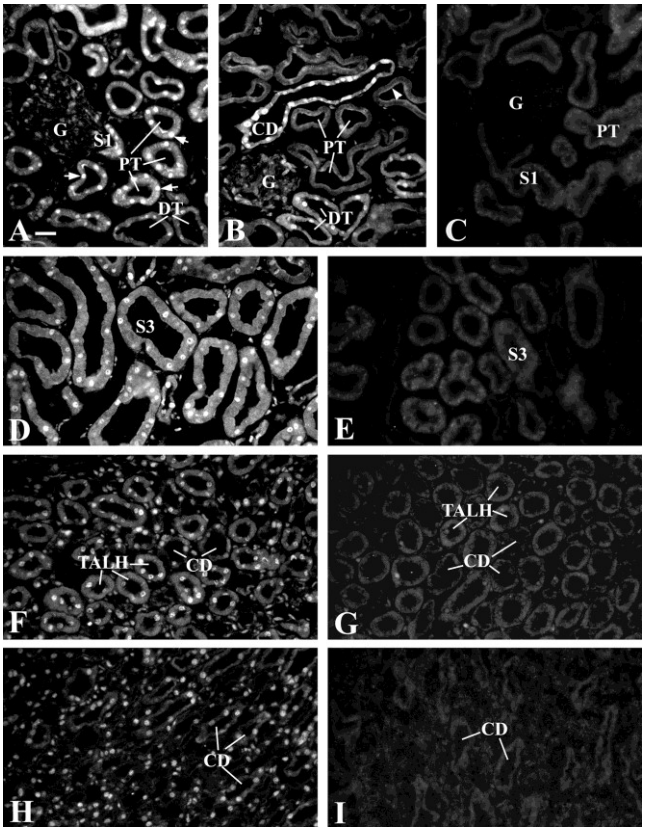
G
S1
PT
DT
A
CD
PT
G
DT
B
G
PT
S1
C
S3
D
S3
E
TALH
CD
F
TALH
CD
G
CD
H
CD
I

Fig. 10.

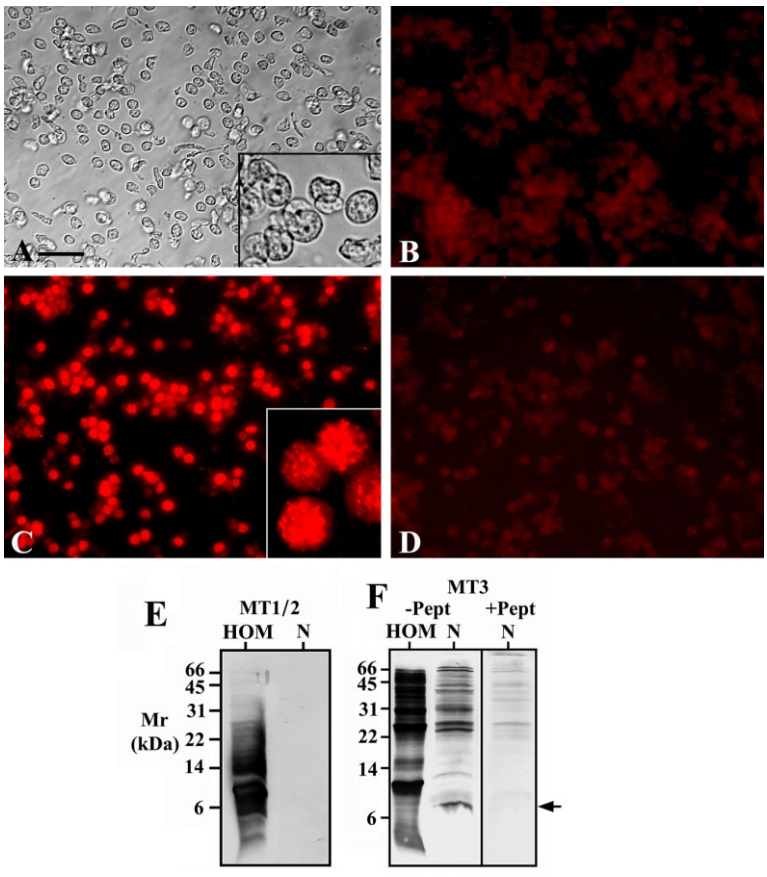
A
B
C
D
E
MT1/2
HOM
N
Mr
(kDa)
66
45
31
22
14
6
F
MT3
-Pept
+Pept
HOM
N
N
66
45
31
22
14
6